Al-Nahrain Journal for Engineering Sciences **NJES** 28(4)573-580, 2025
http://doi.org/10.29194/NJES.28040573

Performance Optimization of Cylindrical WGM Microresonator Sensors for Various Delivery Fiber Diameters

Esraa A. Hassan[1] Alhuda A. Al-mfrji[2] and Aseel I. Mahmood [3]

Authors affiliations:
1) Dept. of Laser and Optoelectronics Engineering, College of Engineering, Al-Nahrain University, Baghdad, Iraq
st.essra.aial.msc@ced.nahrainuniv.edu.iq

2) Dept. of Laser and Optoelectronics Engineering, College of Engineering, Al-Nahrain University, Baghdad, Iraq
alhuda.a.oied@nahrainuniv.edu.iq

3) Scientific Research Commission, Ministry of Higher education and Scientific Research, Baghdad, Iraq.
aseelalzubediy@gmail.com

Paper History:

Received: 10th Dec. 2024

Revised: 7h Apr. 2025

Accepted: 21th Apr. 2025

Abstract

Whispering Gallery Mode Micro-Resonators (WGMRs) have received significant interest due to their great sensitivity to environmental changes, compact size, and ability to operate over a wide spectral range because their low optical losses produce high-quality factors so that they can be used in various sensing applications. This work investigates the design and implementation of cylindrical WGMRs for Refractive Index (RI) sensing for different delivery fiber diameters. Single Mode Fiber with different waist diameters (80,67.1,18) μm were used as delivery fibers. At the same time, the sensor (resonator) fiber is SMF with a diameter (125 μm). Quality factors and Free Spectral Range (FSR) were calculated and analyzed for each diameter. The quality factor for all diameters was in power of 104, which is considered good. The FSR is inversely proportional to fiber diameter. FSR values were (0.678,1.75,2.03) nm for (80,67.1,18) μm delivery fiber diameters respectively. An analyte prepared by NaCl with different refractive indices is used to investigate the RI sensor performance. Higher sensitivity is obtained from the WGMR with a smaller waist diameter, which is (-)74 nm/RIU. While for the delivery fiber diameters (80,67.1) μm were (-0.28, -9.27) nm/RIU respectively. The submitted sensor will have a good contribution in the field of chemical, biological and medical applications.

Keywords: Chemical Etching, FSR, WGMR, Q-Factor, RI Sensor.

تحسين أداء حساسات رنانات أنماط الرواق الهامس الأسطواني لأقطار مختلفة للألياف الناقلة

إسراء عيال حسن، الهدى عبد الحسين عويد، أسيل محمود

الخلاصة:

لقد لاقت رنانات أنماط الرواق الهامس (WGMRs) اهتمامًا كبيرًا بسبب حساسيتها العالية للتغيرات البيئية، وحجمها المدمج، وقدرتها على العمل عبر نطاق طيفي واسع بفضل خسائرها البصرية المنخفضة التي تُنتج عوامل جودة عالية، مما يجعلها قابلة للاستخدام في تطبيقات المتحسسات المختلفة. يتناول هذا العمل تصميم وتنفيذ المستشعرات الأسطوانية من نوع رنانات أنماط الرواق الهامس لتحسس معاملات الانكسار باستخدام أقطار مختلفة للألياف المرسلة. تم استخدام ألياف أحادية النمط بأقطار خصرية (٨٠، ٦٧,١، ١٨) ميكرومتر كألياف ناقلة. في نفس الوقت، كانت ألياف التحسس (الرنانة) من النوع أحادية النمط بقطر (١٢٥) ميكروميتر. تم حساب وتحليل عوامل الجودة ومدى الطيف الحر (FSR) لكل قطر. كانت عوامل الجودة لجميع الأقطار في حدود القوة ١٠٤، وهو ما يُعتبر جيدًا. كان مدى الطيف الحر متناسبًا عكسيًا مع قطر الألياف. كانت قيم المدى الطيف الحر ٠,٦٧٨) ، ١,٧٥، ٢,٠٣ (نانومتر, لأقطار الألياف الناقلة (٨٠، ٦٧,١، ١٨) ميكرومتر على التوالي. تم استخدام محلول تحليلي يحتوي على كلوريد الصوديوم مع معاملات انكسار مختلفة للتحقق من أداء المستشعر. تم الحصول على اعلى حساسية للمستشعر عند استخدام الياف ناقلة ذات قطر خصر أصغر والتي كانت (٧٤-) نانومتر / وحدة معامل انكسار بينما كانت قيم الحساسيات لأقطار الألياف الناقلة (٨٠، ٦٧,١) ميكروميتر هي (٠,٢٨-، ٩,٢٧-) نانومتر / وحدة معامل انكسار على التوالي. سيقدم المستشعر المقدم مساهمة جيدة في مجالات التطبيقات الكيميائية والبيولوجية والطبية.

NJES is an **open access Journal** with **ISSN 2521-9154** and **eISSN 2521-9162**

1. Introduction

The optical micro-resonators that facilitate Whispering Gallery Modes (WGMs) are highly attractive photonic devices because of their narrow spectral linewidths, high quality factors, small mode volumes, and exceptionally high-power densities [1]. WGMs are produced when total internal reflections off the curved surface of the resonator trap light inside the micro-resonator. Because of this reflection, the light inside the curved structure travels along a polygonal path, essentially containing its energy within a relatively tiny volume [2].

WGMs can be supported by a wide range of resonator shapes. The achievable value of the quality factor, ease of manufacture, and ease of integration are typically the three main variables that impact the choice of resonator for a given application. Resonator geometries that include disks, spheres, spheroids, rings, and cylinders can all support WGMs [3-5]. Cylindrical resonators based on optical fibers present unique advantages: they are simple to fabricate, highly uniform in diameter, and offer a simplified optical arrangement that only requires one angular degree of freedom for optimal coupling. This makes the optical setup for experiments involving cylindrical fiber-based micro-resonators more efficient [6]. The ability to tune the spectral positions of WGM The ability to tune the spectral positions of WGM resonances through various external stimuli, such as changes in the surrounding refractive index, mechanical strain, or the application of electric fields, further enhances their utility[7]. A definition of coupling would be the process of introducing light into the micro-resonators and tracking how their characteristics change in response to the sensing event. When the momentum or propagation constant of the input light coincides with a desired cavity mode, the light couples to the micro-resonator[8].Fluorescent coupling, evanescent coupling, and free wave coupling[9]. Efficiency and idealism, which measure the ratio of power actually transmitted to the resonator to total input power and the power transferred to the appropriate excitation mode, respectively, are two key factors that characterize coupling performance. Both of the parameters should be as near to 1 as feasible [10]. The evanescent fields of the WGM resonator and the coupler need to overlap for the coupling to be successful. Effective excitation of resonant modes occurs when phase matching requirements are met[11]. Numerous coupling techniques, including prism coupling [12], tapered fiber [13-15], and integrated waveguide [16, 17]. In this work the tapered fiber coupling technique is used. Usually, a thin fiber taper is used to both excite and probe the WGM resonances. The activation of a WGM results in a spectral drop in the light travelling through the fiber taper [18]. With the help of total internal reflection, light in the form of a WGM travels around the equator while being spatially restricted to a small area close to the surface of the sphere[13]. Due to the advantages of WGMR, they get great interest and wide applications in different fields like biological, chemical, and physical fields [3, 19-25]. This work aims to design and fabricate a cylindrical WGMR based on SMF as a delivery fiber of different waist diameters. The resonator fiber is SMF with a diameter of 125 μm. An analyte of different RIs made from NaCl was used to change the RI of the surrounding sensor.

2. Experimental Work

The cylindrical structure is built using commercially available SMF. The core-cladding/ diameter of SMF is 8/125μm. SMF with FC connectors that are 50cm long have been used as delivery fiber. To reduce the delivery fiber diameter, the SMF's polymer protective layer of the middle region is stripped using a mechanical stripper.

Then, it was cleaned using acetone with a purity of 99% to remove all polymer residue. The striped region is about 3cm in length. Then, this region is fixed in a square-shaped cell fabricated from PMMA (Poly Methyl Meth Acrylate) with a dimension of 5×5cm, the groove dimensions length 5 cm, wide 5 cm, depth 1 mm. The chemical etching process is used to reduce the optical fiber diameter. For this purpose, diluted HF acid (Hydrofluoric) is used. The original concentration of HF is 42%, and it is diluted using distilled water (DW) with a ratio (of 3:1). Due to our observations, the diluted HF acid etched the optical fiber more gradually and uniformly, permitting better control over the etching depth and surface finish. Concentrated acid can etch too aggressively, surface roughness, irregular geometries, and risk of over-etching or damaging the fiber core. The diluted acid is added to the cell groove, and the stripped optical Fiber is fixed. The designed cell allows to make all the parts of optical fiber etched by HF acid equally. The SMF is connected to the optical laser source coupled with fiber (EITELONG Ins., SAT-3E), the stripped region is immersed into the acid container, and the other side of the SMF is connected to the optical power meter (EITELONG Ins, SAT-3E).

The laser source has three nm input wavelengths (1550, 1310, and 850). The 1550 nm wavelength was chosen in this experiment. First, the optical power was recorded before adding the HF acid, and then it was measured every 1 minute till the desired diameter was obtained. Fig. 1 shows the experimental setup of the chemical etching technique.

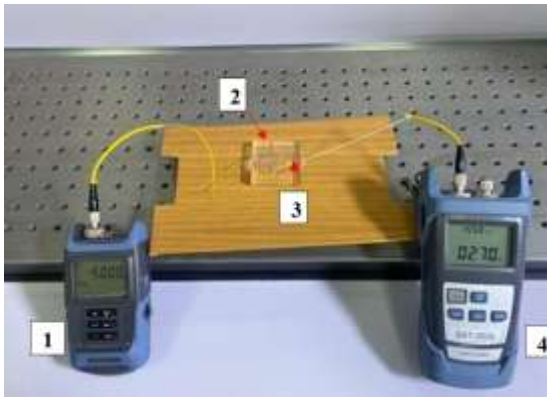

Figure (1): The experimental setup of the chemical etching experiment, (1) optical source, (2) Optical fiber immersed in acid, (3) PMMA cell, and (4) optical power meter.

The chemical etching process takes different times to get different waist diameters. SMF's chemical etching process time is (270, 150, and 90) minutes. Then distilled water is used to clean the fiber and cells. The cleaning step is repeated many times to ensure all acid residue is removed. Furthermore, to stop the chemical reaction process. The outer diameter of the sample was then measured using an optical microscope (Nikon Eclipse ME600) with a magnification of 100X. The final diameters for SMF with etching time (270, 150, and 90) were (18, 67.1, and 80) μm, respectively. Fig. 2 shows the microscopic image of the manufactured delivery fibers of different diameters.

After preparing single-mode fibers (SMFs) with tapered waist diameters of 18 μm, 67.1 μm, and 80 μm for use as delivery fibers and selecting an untampered SMF with a standard cladding diameter of 125 μm as the resonator fiber, the two fibers were arranged perpendicularly to form a cylindrical Whispering Gallery Mode Resonator (WGMR) structure. As described earlier, this configuration was assembled within a polymethyl methacrylate (PMMA) cell.

To characterize the system, one end of the delivery fiber was connected to an Amplified Spontaneous Emission (ASE) broadband light source with an operational bandwidth of 1525–1565 nm, while the opposite end was coupled to an Optical Spectrum Analyzer (OSA) operating over the same wavelength range. Spectral data were acquired in real time using the accompanying OSA software. Initially, the optical spectrum of the structure was recorded prior to coupling (i.e., before fixing the sensor fiber in place). Subsequently, the spectrum was measured again after establishing the coupling to confirm successful mode excitation within the WGMR.

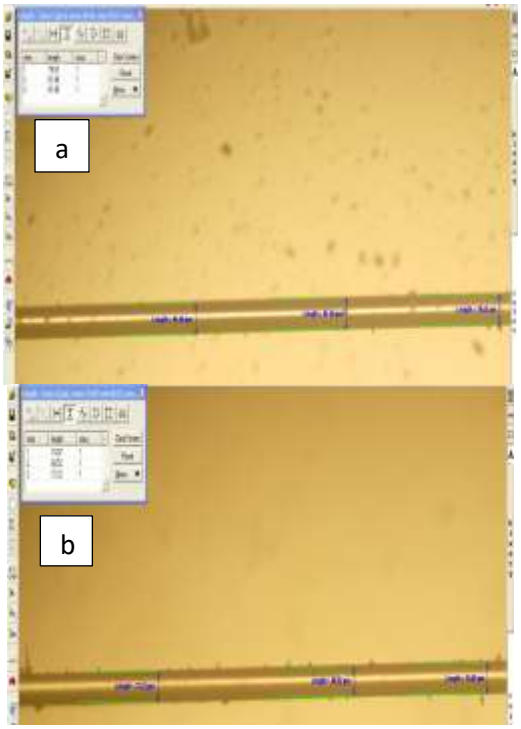

Figure (2): Microscopic image of delivery fibers with diameters, (a) SMF- 80μm, (b) SMF- 67.1μm, (c) SMF- 18μm.

To tune the optical spectrum of the WGMR, the surrounding refractive index is changed. Two different liquids with different refractive indices are used. An analyte is used to apply the WGMR as a refractive index sensor, which is food salt (NaCl) with refractive indices values (1.345,1.35,1.356,1.361,1.366) RIU. Fig. 3 shows the photographic image and schematic diagram of the WGMR refractive index sensor.

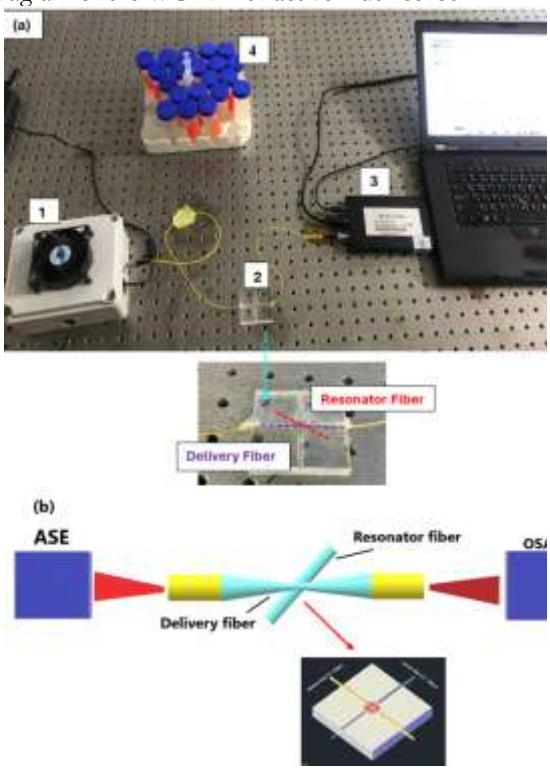

Figure (3): (a) Experimental set up photographic images where (1) light source, (2) WGMR, (3) OSA with PC, and (4) analytes. (b) The schematic diagram of the experiment.

3. Results and Discussions

The optical fiber diameter decreases with increasing etching time as it clears in Fig. 2. The rate of chemical reaction between the etchant and the fiber material determines the link between etching time and fiber waist diameter. This reaction can be affected by temperature, HF acid concentration, and the characteristics of the fiber material. The transmission spectra for the produced delivery fibers were recorded and analyzed as shown in Fig. 4.

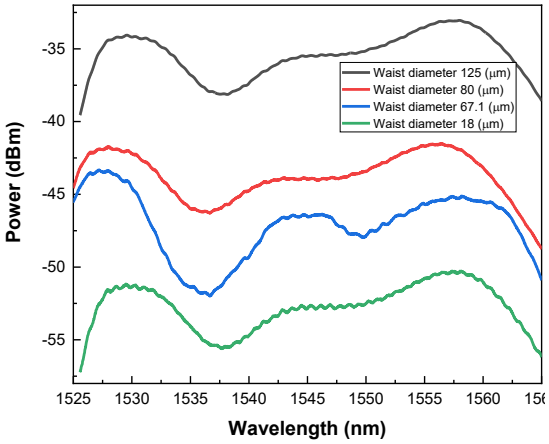

Figure (4): The transmission spectra of SMF delivery Fiber after chemical etching of different time.

Reducing the diameter of SMFs through chemical etching can have significant effects on their transmission spectra as it clear in Fig. 4. These effects arise due to changes in the fiber's physical structure, which in turn affect how light propagates through the fiber. A smaller fiber diameter enhances the evanescent field, where more light interacts with the surrounding medium. This can be beneficial for sensing applications.

First, the optical spectrum of the submitted structure before coupling (no WGM) and after coupling (WGMR) is collected and analyzed. Fig.5 shows the transmission spectra before and after coupling for different SMF delivery diameters.

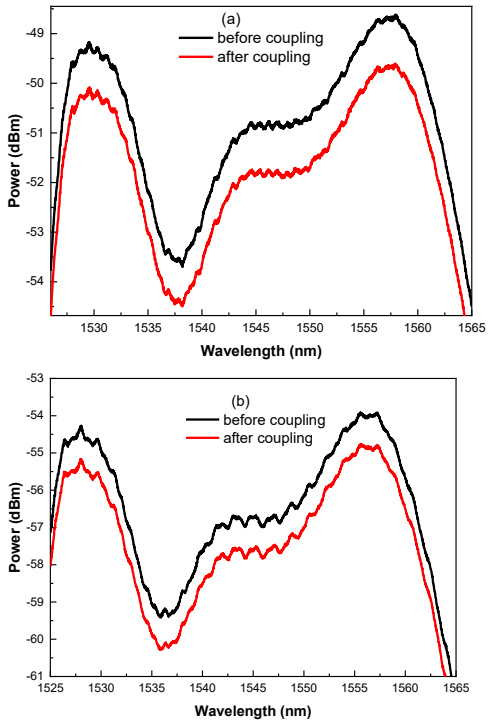

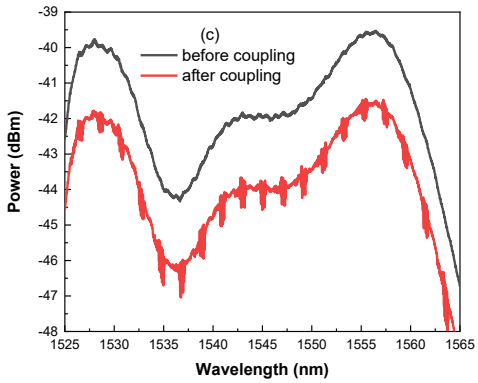

Figure (5): The transmission spectra of submitted structure before and after coupling for different SM delivery fiber diameters, (a) 80 μm, (b) 67.1 μm, and (c) 18 μm.

Before the coupling process, the spectrum was relatively smooth, and there were very tiny dips because of the loss due to the chemical etching process. After coping with a cylindrical structure, defined dips appear. Coupling efficiency plays a crucial role and may lead to variation in the amplitude and shape of dips. The dips become clearer and defined when the diameter of the delivery fiber is reduced. This means more power transfer from the delivery Fiber to the resonator Fiber, and the coupling efficiency is good. The optical properties of the manufactured WGMR are studied and analyzed. Q-Factor, and FSR as illustrated in Fig's. (6, 7) respectively.

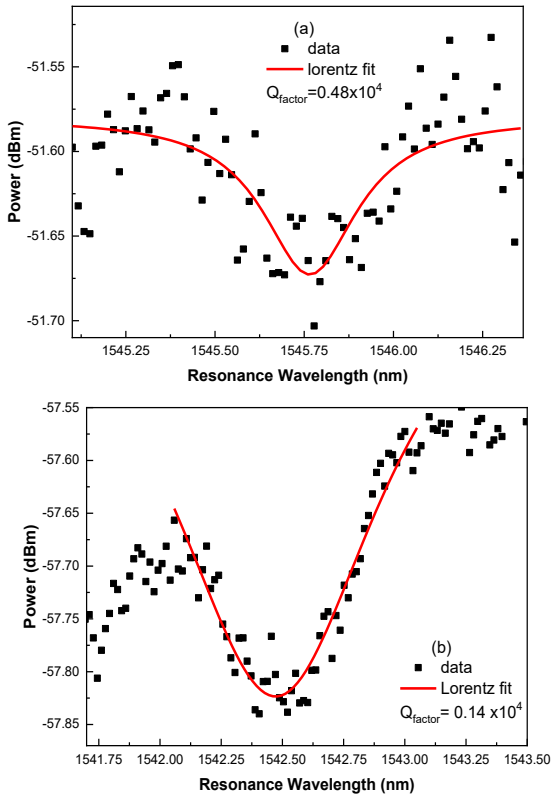

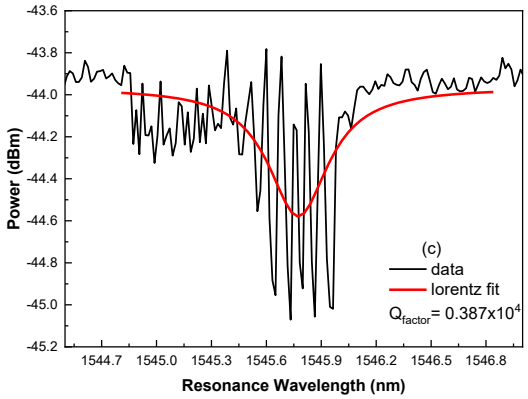

Figure (6): The Q -Factor of submitted structure for different SM delivery Fiber diameters, (a) 80µm, (b) 67.1µm, and (c) 18µm.

The quality factor and FSR of the WGM resonance are all influenced by the coupling efficiency between the delivery fiber and the microresonator, which is directly impacted by the waist diameter of the delivery fiber. The quality factor Q can be determined from the WGM spectrum as [26]:

$$Q = \frac{\omega_\circ}{\delta\omega} = \frac{\lambda_\circ}{\delta\lambda} \qquad (1)$$

Where $(\lambda_\circ)$ $(\omega_\circ)$ is the resonance frequency (wavelength), and $(\delta\omega)$ $(\delta\lambda)$ is the line width (Full Width at Half Maximum, FWHM) of the resonant mode. Based on the numbers and curves, the Q_{Factor} remains at 10^4. A relationship that is reversible between FSR and resonator diameter lowering the resonator diameter makes the dips more noticeable and distinct, resulting in a greater FSR. Lastly, finesse, which characterizes the resonator's spectrum resolution, is dependent on FSR levels and exhibits similar characteristics.

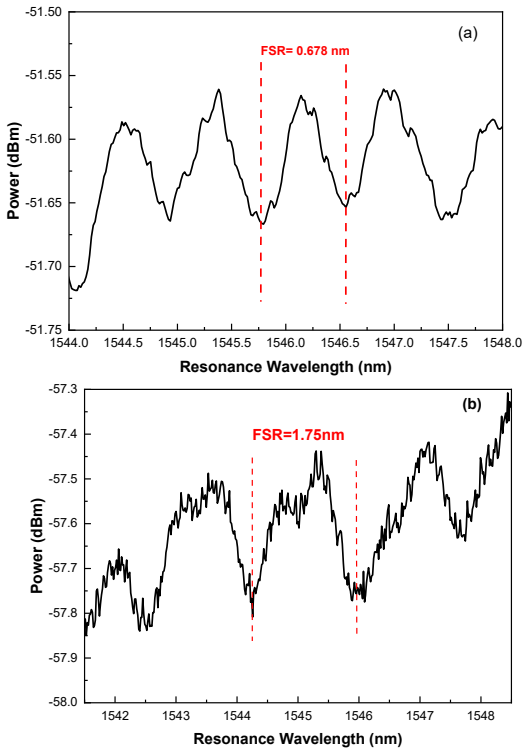

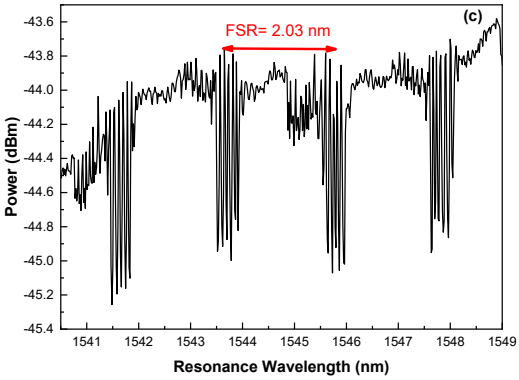

Figure (7): The FSR of submitted structure for different SM delivery Fiber diameters, (a) 80µm, (b) 67.1µm, and (c) 18µm.

To study the sensor performance with different delivery fiber waist diameters, analytes prepared from food salt (NaCl) with refractive indices values (1.345,1.35,1.356,1.361,1.366) RIU is used. Fig. 8 shows WGM spectra excited with a broadband laser source tuned due to the variation of surrounding refractive indices.

The wavelength shifting of light inside the resonator is determined by the effective optical path length, which is influenced by the refractive index of the surrounding medium. When the refractive index increases, the effective path length decreases, leading to a blue shift in the resonant wavelengths. Also, the phase velocity decreases when the refractive index increases, reducing the effective path length. Another reason for the blue shift could be the increase in the surrounding refractive index. Changes in the refractive index can redistribute the electromagnetic field around the resonator. This redistribution affects the coupling conditions and alters the resonant modes, causing a blue shift in the spectrum. The WGMR's resonant mode and the fiber mode's evanescent field overlap tuned, resulting in effective energy transmission. In this work, the observed Q factor was relatively low (10^4), contributing to a limited sensitivity of the WGMR. However, the sensitivity could be significantly enhanced by achieving higher Q factors. High-quality resonances are essential for improving the device's response to environmental changes, such as variations in the refractive index or the presence of analytes. Achieving optimal coupling conditions is a key factor in realizing high-Q resonances. In this regard, it was observed that decreasing the waist diameter of the delivery fiber improves coupling efficiency, which in turn enhances the sensor's sensitivity. Consequently, this improvement in sensitivity could also lead to better resolution in detection.

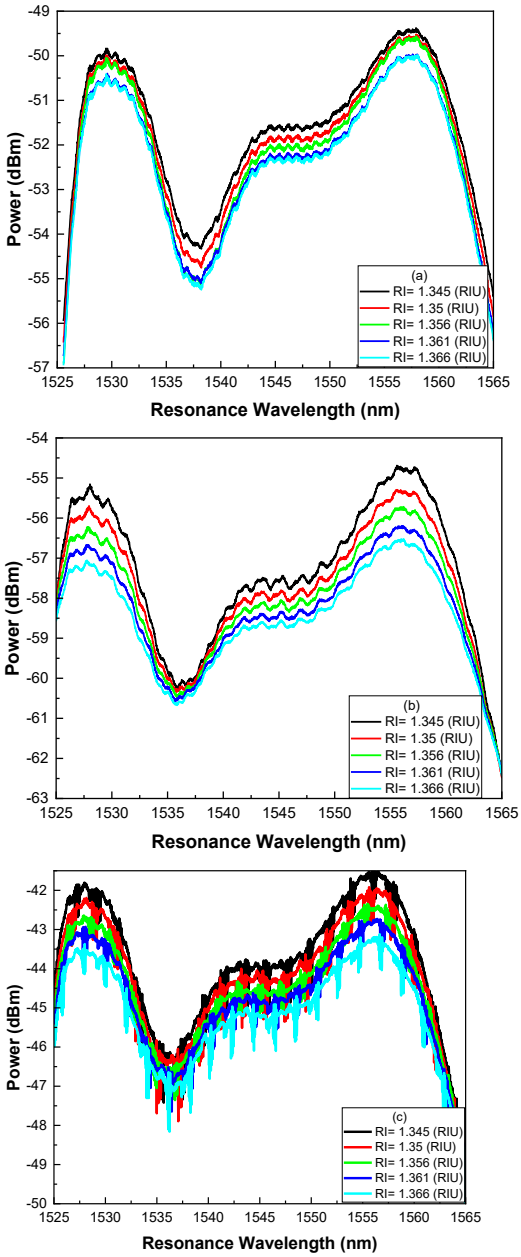

Figure (8): The resonance spectra of WGMR-RI sensor using delivery fiber of waist diameters, (a) 80µm, (b) 67.1µm, and (c) 18µm.

The relationship between the resonance wavelength shifting due to changing of surrounding RI (Sensitivity) is illustrated in Fig. 9 for WGMR with delivery Fiber with different waist diameters (80,67.1,18) µm. The sensitivity (S) of the WGMR sensor is calculated using the following equation [8]:

$$S = \frac{\Delta\lambda_{res}}{\Delta RI_n} \qquad (2)$$

Where $\Delta\lambda_{res}$ is the difference in resonance wavelength, and ΔRI_n is the variation in analyte surrounding RI.

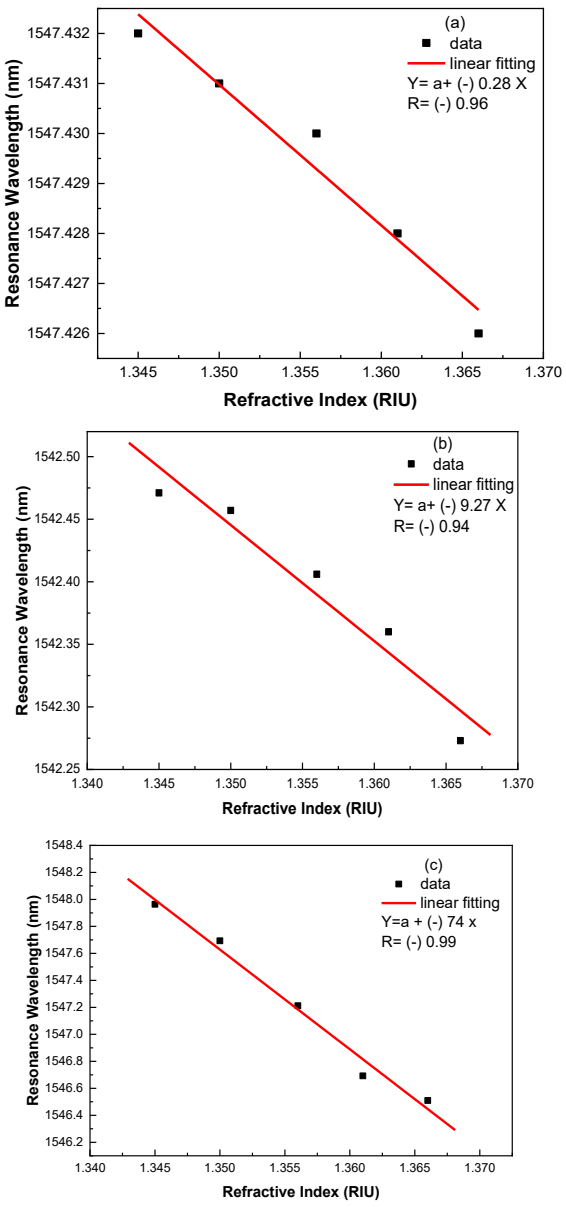

Figure (9): Resonance wavelength shifting versus analyte RI's for WGMR SM delivery Fiber of waist diameter, (a) 80µm, (b) 67.1µm, (c) 18µm.

4. Conclusions

This work demonstrated a cylindrical WGMR structure using single-mode delivery fibers with varying waist diameters, achieved through a controlled chemical etching process. The etching rate, governed by the reaction between hydrofluoric acid (HF) and the fiber material, plays a crucial role in determining the final waist diameter of the delivery fiber. A clear inverse relationship was observed between the resonator diameter and the FSR, with smaller resonator diameters leading to more widely spaced and pronounced resonance dips. Additionally, the resonance behavior of the WGMR was shown to be tunable by modifying the surrounding refractive index, emphasizing its potential for refractive index sensing. Notably, using smaller delivery fiber diameters enhances the evanescent field interaction, thereby improving sensitivity to environmental changes. Although the Q-factor observed in this study was modest, further optimization could significantly

enhance sensitivity and resolution. Overall, the proposed WGMR structure exhibits promising potential for biochemical and medical sensing applications, particularly with future Q-factor and coupling efficiency improvements.

Funding

"The authors declare that no funds, grants, or other support were received during the preparation of this manuscript."

Competing Interests

"The authors have no relevant financial or non-financial interests to disclose."

Author Contributions

"All authors contributed to the study conception and design. Material preparation, data collection and analysis were performed by Esraa A. Hassan, Alhuda A. Al-Mfrji and Aseel I. Mahmood. The first draft of the manuscript was written by Esraa A. Hassan and all authors commented on previous versions of the manuscript. All authors read and approved the final manuscript."

Research Data Policy and Data Availability Statements

My manuscript has no associated data.

7. References:

[1] S. Hao and J. Su, "Whispering gallery mode optical resonators for biological and chemical detection: current practices, future perspectives, and challenges," Rep. Prog. Phys., vol. 87, no. 6, 2024. https://doi.org/10.1088/1361-6633/ad99e7

[2] L. Huang, Optical Whispering-Gallery Mode Spectroscopy for the Study of Molecule Adsorption and Desorption, Ph.D. dissertation, Rutgers The State Univ. of New Jersey, School of Graduate Studies, 2011.

[3] N. Toropov, G. Cabello, M. P. Serrano, R. R. Gutha, M. Rafti, and F. Vollmer, "Review of biosensing with whispering-gallery mode lasers," Light: Sci. Appl., vol. 10, p. 42, 2021. https://doi.org/10.1038/s41377-021-00471-3

[4] A. François, Y. Zhi, and A. Meldrum, "Whispering gallery mode devices for sensing and biosensing," in Photonic Materials for Sensing, Biosensing and Display Devices, pp. 237-288, 2016. https://doi.org/10.1007/978-3-319-24990-2_9

[5] Y. C. Chen and X. Fan, "Biological lasers for biomedical applications," Adv. Opt. Mater., vol. 7, p. 1900377, 2019. https://doi.org/10.1002/adom.201900377

[6] V. Kavungal, A. K. Mallik, G. Farrell, Q. Wu, and Y. Semenova, "Strain-induced spectral tuning of the whispering gallery modes in a cylindrical micro-resonator formed by a polymer optical fiber," Appl. Opt., vol. 56, pp. 1339-1345, 2017. https://doi.org/10.1364/AO.56.001339

[7] A. Mahmood, V. Kavungal, S. S. Ahmed, G. Farrell, and Y. Semenova, "Magnetic-field sensor based on whispering-gallery modes in a photonic crystal fiber infiltrated with magnetic fluid," Opt. Lett., vol. 40, pp. 4983-4986, 2015. https://doi.org/10.1364/OL.40.004983

[8] L. Cai, J. Pan, and S. Hu, "Overview of the coupling methods used in whispering gallery mode resonator systems for sensing," Opt. Lasers Eng., vol. 127, p. 105968, 2020. https://doi.org/10.1016/j.optlaseng.2019.105968

[9] H. Yu, X. Liu, W. Sun, Y. Xu, X. Liu, and Y. Liu, "A brief review of whispering gallery mode in sensing," Opt. Laser Technol., vol. 177, p. 111099, 2024. https://doi.org/10.1016/j.optlastec.2024.111099

[10] Y. Zheng, Z. Wu, P. P. Shum, Z. Xu, G. Keiser, and G. Humbert, "Sensing and lasing applications of whispering gallery mode microresonators," Opto-Electron. Adv., vol. 1, p. 180015, 2018.

[11] Y. Zhang, Q. Song, D. Zhao, X. Tang, Y. Zhang, and Z. Liu, "Review of different coupling methods with whispering gallery mode resonator cavities for sensing," Opt. Laser Technol., vol. 159, p. 108955, 2023. https://doi.org/10.1016/j.optlastec.2022.108955

[12] M. R. Foreman, F. Sedlmeir, H. G. Schwefel, and G. Leuchs, "Dielectric tuning and coupling of whispering gallery modes using an anisotropic prism," J. Opt. Soc. Am. B, vol. 33, pp. 2177-2195, 2016. https://doi.org/10.1364/JOSAB.33.002177

[13] Y. Li, O. Svitelskiy, D. Carnegie, E. Rafailov, and V. N. Astratov, "Evanescent light coupling and optical propelling of microspheres in water immersed fiber couplers," in Proc. Laser Resonators, Microresonators, and Beam Control XIV, 2012, pp. 316-323. https://doi.org/10.1117/12.908405

[14] Y. Mei, D. Wang, Q. Wang, and Y. Zhang, "All optical fiber dual WGM resonators," IEEE Photon. Technol. Lett., 2024. https://doi.org/10.1109/LPT.2024.3507697

[15] X. Luo, H. Li, W. Wang, Y. Song, and L. Zhu, "Tapered-optical fiber tip coupler for capillary whispering gallery mode," Opt. Eng., vol. 63, p. 026103, 2024. https://doi.org/10.1117/1.OE.63.2.026103

[16] Y. Mei, D. Wang, Q. Wang, and Y. Zhang, "Optical fiber integrated WGM cylindrical cavity resonator," Opt. Lett., vol. 49, pp. 4609-4612, 2024. https://doi.org/10.1364/OL.528812

[17] L. J. Roche, F. Betz, Y. Yang, I. Limame, C. W. Shih, and S. Burger, "Numerical investigation of a coupled micropillar-waveguide system for integrated quantum photonic circuits," Adv. Quantum Technol., p. 2400195, 2024. https://doi.org/10.1002/qute.202400195

[18] F. Azeem, M. R. Chaudhry, M. S. Anwar, H. A. Khan, L. Ma, and A. D. Khan, "Optical whispering gallery mode resonators: analysing thermo-optic tuning in a silicon sphere," J. R. Soc. N. Z., pp. 1-25, 2024. https://doi.org/10.1080/03036758.2024.2395909

[19] D. Kazanov and A. Monakhov, "Open whispering gallery mode resonators," Opt. Lett., vol. 49, pp. 6577-6580, 2024. https://doi.org/10.1364/OL.540748

[20] P. George, A. Saritha, and A. Ramachandran, "Whispering gallery mode based micro-ring resonator for magnetic field sensing," Appl. Opt., vol. 63, pp. 5796-5801, 2024. https://doi.org/10.1364/AO.528974

[21] M. Adolphson, Optimization and Applications of Whispering Gallery Mode Microbubble Resonator, 2024. https://doi.org/10.3791/66890

[22] N. Aravantinos-Zafiris and M. M. Sigalas, "Acoustic whispering gallery modes in a split ring resonator," 2024.

[23] L. Cai, S.-w. Li, F.-c. Xiang, J. Liu, and Q. Liu, "Fano resonance in whispering gallery mode microcavities and its sensing applications," Opt. Laser Technol., vol. 167, p. 109679, 2023. https://doi.org/10.1016/j.optlastec.2023.109679

[24] J. Su, "Label-free biological and chemical sensing using whispering gallery mode optical resonators: past, present, and future," Sensors, vol. 17, p. 540, 2017. https://doi.org/10.3390/s17030540

[25] Y. Wang, S. Zeng, G. Humbert, and H. P. Ho, "Microfluidic whispering gallery mode optical sensors for biological applications," Laser Photon. Rev., vol. 14, p. 2000135, 2020. https://doi.org/10.1002/lpor.202000135

[26] W. Mao, Y. Li, X. Jiang, Z. Liu, and L. Yang, "A whispering-gallery scanning microprobe for Raman spectroscopy and imaging," Light: Sci. Appl., vol. 12, p. 247, 2023. https://doi.org/10.1038/s41377-023-01276-2

.